PHILOSOPHICAL TRANSACTIONS OF THE ROYAL SOCIETY A MATHEMATICAL, PHYSICAL & ENGINEERING SCIENCES

The Shelf-Sea Fronts: Implications of their Existence and Behaviour [and Discussion]

J. H. Simpson, D. J. Crisp and C. Hearn

Phil. Trans. R. Soc. Lond. A 1981 **302**, 531-546
doi: 10.1098/rsta.1981.0181

Phil. Trans. R. Soc. Lond. A **302**, 531–546 (1981)
Printed in Great Britain

The shelf-sea fronts: implications of their existence and behaviour

By J. H. Simpson
Marine Science Laboratories, University College of North Wales, Menai Bridge, Anglesey LL59 5EY, U.K.

[Plates 1 and 2]

This paper reviews the results of recent observations of the shelf-sea fronts and discusses the relation of these features to what is known of the mean circulation. Evidence from satellite infrared imagery and ship data are presented to illustrate the movements and structure of the fronts. Many of the data can be rationalized in terms of models of tidal mixing based on vertical exchange only, with a feedback element, which is needed to account for the small observed adjustment to the springs–neaps stirring cycle.

The density gradients within the front imply strong geostrophic currents along the isobars but the available evidence does not support the idea of a frontal jet. The complicated velocity field observed may be the result of large-scale (20–40 km) eddies that develop from instability of the flow.

The relative success of local energy models implies that horizontal advection normal to the fronts is weak. A simple model of depth-uniform advection indicates that frontal positions and gradients should be sensitive to flows as small as 1 cm s^{-1}, and two examples of such influence are tentatively identified.

1. Introduction

Over the continental shelf tidal flows exert strong frictional stresses on the seabed. In stress terms, these tidal streams are equivalent to hurricane-force winds in the atmosphere blowing regularly twice per day. As well as playing an important part in the tidal dynamics, these stresses serve to produce turbulent kinetic energy which is responsible for vertical mixing.

Variations in the level of tidal stirring divide the shelf seas, during the summer régime, into well mixed and stratified zones separated by high gradient regions called fronts. The spatial distribution of mean energy dissipation in the tidal streams, which is determined by the response of the shelf seas to forcing by the ocean tide, is essentially constant and so, therefore, are the geographical positions of the fronts which make only relatively small excursions from their mean positions.

Energy arguments (presented in § 3) may be used to describe the competition between the agencies tending to stabilize the water column (surface heat and freshwater), and stirring mechanisms (tidal streams and wind) that promote vertical mixing. For the simplest case (Simpson & Hunter 1974), which involves only heating (at rate $\dot{Q}$) and stirring by a tidal stream of amplitude u, the controlling parameter is found to be $\dot{Q}h/u^3$ where h is the water depth. Where $\dot{Q}$ may be regarded as spatially uniform, the quantity h/u^3 becomes the main determinant of stratification and frontal position.

Surface stress, applied by the wind, is usually also an important influence on vertical structure but, in the shelf seas around the U.K., the tidal flows generally predominate and control the

pattern of structure. This predominance of tide over wind-stirring represents a useful simplification of the problem and has made the U.K. shelf a particularly fruitful area for study. From the early surveys of Matthews (1913), the partitioning of the Irish Sea into mixed and stratified zones was clear, and Dietrich (1951), on the basis of observed structure in the English Channel, pointed to the importance of tidal streams in controlling mixing. It is, however, in the intensified effort of the last decade that the ordering of vertical structure in the shelf seas has become fully apparent. Progress has been facilitated by the advent of high quality infrared (i.r.) imagery which has provided synoptic pictures of sea surface temperature over large areas of the shelf confirming and greatly extending the results of ship surveys.

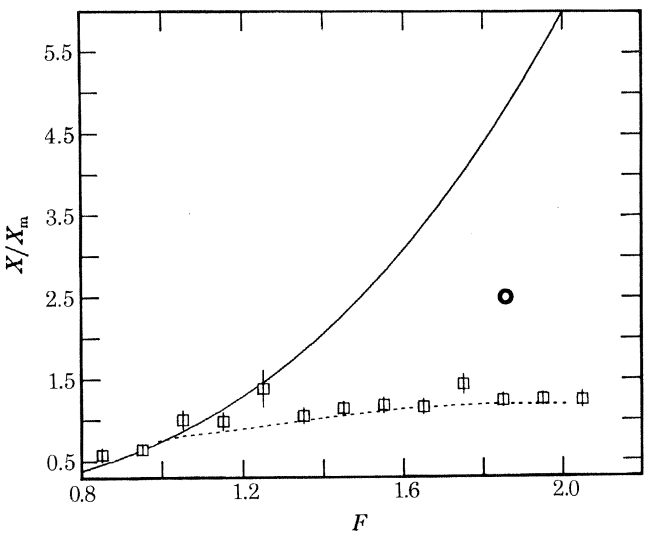

FIGURE 2. Summary of frontal displacement data plotted against the tidal range factor F. The data refer to displacements of the fronts along reference lines (Simpson & Bowers 1981) approximately perpendicular to the fronts. Results are presented in terms of the ratio X/X_m where $X = h/u^3$ at the observed tidally corrected position and X_m is the mean value of h/u^3 for the front concerned.

Over 400 points determined in this way from images are shown here in the form of mean values for each interval of 0.1 in F. The vertical error bars represent the standard error $s = \sigma/\sqrt{n}$ where σ = standard deviation of the normalized displacement and n is the number of observations in the class. The continuous curve represents the equilibrium adjustment condition in which the heating and stirring are in balance. The open circle indicates the limit of adjustment predicted by equation (4).

In this paper I shall first attempt to summarize the results of i.r. investigations and other recent observational results on the structure of fronts and assess to what extent they can be understood in terms of local energy models of mixing processes that neglect advective effects. Consideration will then be given to the relation between fronts and circulation, both in terms of the internal circulation inherent in fronts, and the possible reaction of fronts to imposed mean flows.

2. Observations of fronts

(a) *Frontal positions*

Although it was first demonstrated by specific ship surveys and reference to historical T–S data (Simpson & Hunter 1974, Simpson *et al.* 1977) that fronts occupy nearly consistent positions in the shelf seas, it is certainly satellite i.r. data that have served to illustrate this property of the fronts

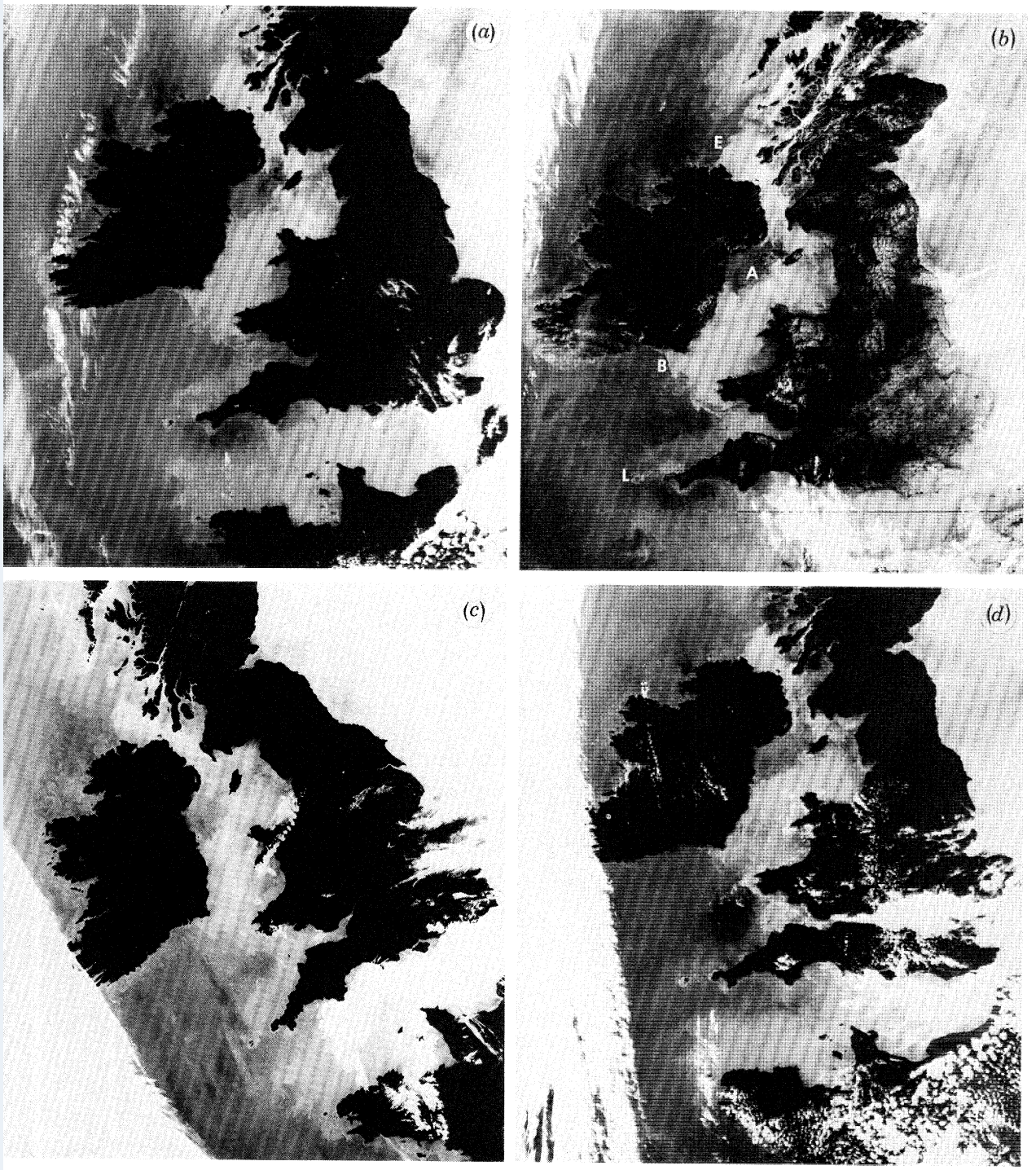

FIGURE 1. Satellite infrared images of the U.K. shelf area in May 1980. (*a*) TIROS–N, 16.v.80, 15h29 G.M.T.; (*b*) NOAA–6, 16.v.80, 19h01 G.M.T.; (*c*) NOAA–6, 17.v.80, 08h49 G.M.T.; (*d*) TIROS–N, 17.v.80, 15h18 G.M.T.

Letters on (*b*) indicate the principal frontal zones referred to in the text: A, western Irish Sea front; B, Celtic Sea front; E, Islay front; L, Scilly Isles.

(*Facing p.* 532)

PHILOSOPHICAL TRANSACTIONS OF THE ROYAL SOCIETY A MATHEMATICAL, PHYSICAL & ENGINEERING SCIENCES

FIGURE 9. Enlarged satellite infrared image of the Scilly Isles region from NOAA–5 at 10h28 G.M.T. 20.viii.76.

PHILOSOPHICAL TRANSACTIONS OF THE ROYAL SOCIETY A MATHEMATICAL, PHYSICAL & ENGINEERING SCIENCES

most clearly. In spite of cloud interference, a large archive of images, which show the spatial continuity and persistence of fronts, is being accumulated. In these images the shelf-sea fronts are identified by sharp changes in sea surface temperatures which, for much of the year, represent the largest gradients present. Figure 1 (plate 1) is a selected group of images from May 1980 in which cloud interference is minimal so that the persistence of the various labelled frontal features may be clearly seen.

Imagery of this kind has permitted studies of the small displacements of the fronts relative to their mean positions. Such movements may result from simple tidal advection or adjustments due to changes in the stirring and heating rates. In particular the large change in stirring rate ($\propto U^3$) over the fortnightly neaps–springs cycle has been proposed as a likely cause of frontal adjustment (see, for example, Pingree *et al.* 1977).

Figure 2 shows a summary of the results from recent studies of frontal movement (Simpson & Bowers 1979, 1981) based on the NOAA-5 and TIROS-N archives. The tidally corrected displacement data from different frontal zones observed in about 120 separate images are combined in

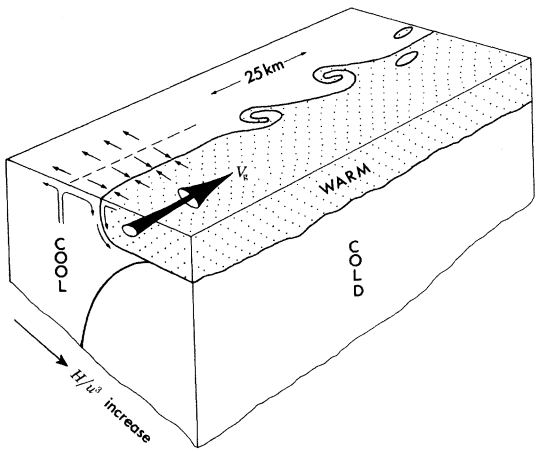

FIGURE 3. Schematic diagram of frontal structure based on ship and satellite observations. The along-front flow V_g required to balance the density gradients is not generally observed, probably because of the development of instabilities. The vertical plane circulation suggested is based on indirect evidence from the temperature field and observations of a convergent zone near to the maximum in horizontal temperature gradient.

a plot of the parameter h/u^3 at the observed frontal position against the tidal range factor F (ratio of tidal range to the range at mean neaps). The F-values were those applying two days before the observation, a time lag that gives the maximum correlation. This indicates that the greatest advance of the front into the stratified water occurs two days after spring tides. The magnitude of the displacement is however small and only a fraction of the 'equilibrium adjustment', which is the movement required to maintain a balance between heating and stirring at the front.

For representative gradients of h/u^3, the observed adjustment is equivalent to a movement of *ca.* 4 km in frontal position, which is less than the residual r.m.s. displacement of *ca.* 7 km that remains after the removal of the fortnightly trend. No significant reduction in the variance can be achieved by consideration of seasonal effects; once established in May the fronts show no systematic change in mean position with time. Nor is there any evidence of the direct response of frontal positions to wind-forcing.

PHILOSOPHICAL TRANSACTIONS OF THE ROYAL SOCIETY A MATHEMATICAL, PHYSICAL & ENGINEERING SCIENCES

(*b*) *Structure of fronts*

The density configuration of a typical shelf-sea front is shown schematically in figure 3. At high h/u^3 the density profile generally consists of two layers separated by a sharp pycnocline, while in the low h/u^3 region properties are almost uniform throughout the column. At the boundary, strong horizontal density gradients of opposite sign occur in the upper and lower layers. Associated with these gradients, there should be an along-front quasigeostrophic flow (a frontal jet) with maximum velocity differences of *ca.* 30 cm s^{-1} in the residual current which should be directed parallel to the front.

A study of the Islay front west of Scotland (see figure 1) has produced evidence of strong flow of this kind (*ca.* 20 cm s^{-1}) along the front, although the observed vertical shear was not in precise geostrophic balance with the density field (Simpson *et al.* 1979). Evidence from other fronts, however, suggests a more complex picture which is frequently not amenable to interpretation in terms of quasigeostrophic flows parallel to the front (Simpson *et al.* 1978).

The apparent complexity of the flow may be a consequence of large-scale disturbances which are, at times, observed in infrared images (Simpson & Pingree 1977) and which may be responsible for the residual r.m.s. displacement in frontal positions noted above. It has been suggested (Pingree 1978) that these features may be interpreted in terms of eddies resulting from baroclinic instability. In this picture an initial perturbation of the along-front flow grows as a wave-like disturbance which eventually curls up, usually in the same sense as the Earth's rotation. The scale of these disturbances is in the range 20–40 km which is larger than the wavelength λ_E of the fastest growing wave predicted by the stability analysis of Eady which gives

$$\lambda_E = 4R_d = 4(g'D)^{\frac{1}{2}}/f \approx 16\,\text{km}$$

where R_d is the Rossby radius of deformation based on the reduced gravity g' and surface layer depth D in the stratified water, and f is the Coriolis parameter.

While this scale prediction may be considered as suggestive of the baroclinic nature of these instabilities, other processes may contribute. Some of the energy in these eddies may be drawn from the kinetic energy of the flow including that due to the tidal component. Such instabilities would not be confined to frontal areas but would tend to be preferentially observed there because of the strong surface temperature signal. Even at fronts the positive identification of evolving eddies is difficult and in only a few cases do we have a convincing sequence of cloud-free images on which to base estimates of time-scales (*ca.* 3 days).

Our knowledge and understanding of these eddies is therefore still sketchy and they remain as a major challenge for future studies. Their likely importance as a mechanism for cross-frontal mixing has been discussed by Pingree (1978) on the basis of an analogy with the atmospheric eddy transport theory of Green (1970). The interchange of water across frontal boundaries in this way is one of the candidate mechanisms for increased biological activity in frontal zones, a possibility discussed by Holligan (this symposium).

While satellite i.r. data have given us a new perspective of horizontal temperature fields, more detailed pictures of the vertical structure in fronts have emerged from profiling work with undulating CTDs. As well as permitting rapid surveys of frontal regions, these instruments have improved horizontal resolution and reduced the scale of aliasing which is implicit in the interpolation between widely separated stations.

Figure 4 (from Allen *et al.* 1980) illustrates the structure of the western Irish Sea front with

PHILOSOPHICAL TRANSACTIONS OF THE ROYAL SOCIETY A MATHEMATICAL, PHYSICAL & ENGINEERING SCIENCES

horizontal and vertical resolutions of less than 500 m and *ca.* 1 m respectively. The pycnocline, in this example in July, is seen to incline upwards with a slope of *ca.* 1:500, outcropping at the surface in a region where the maximum surface gradient exceeds 1.5 °C km^{-1}. Close to this point on the mixed side of the front, there is a minimum in surface temperature with an associated upward displacement of the 10, 10.5 and 11 °C isotherms. The occurrence of this minimum is common to many sections obtained with the undulating CTD and is frequently observed in ships' thermograph data. It is suggestive of the upwelling of cold water from the lower layer on the stratified side of the front as indicated schematically in figure 3.

Also shown are the convergence and downwelling whose occurrence is suggested by the accumulations of surface material frequently found in the region of maximum gradient.

3. Energetics of mixing

(*a*) *Model without advection*

Much of what we know about fronts and their behaviour can be understood in terms of basic energy considerations, which were presented in Simpson & Hunter (1974) and Simpson *et al.* (1978).

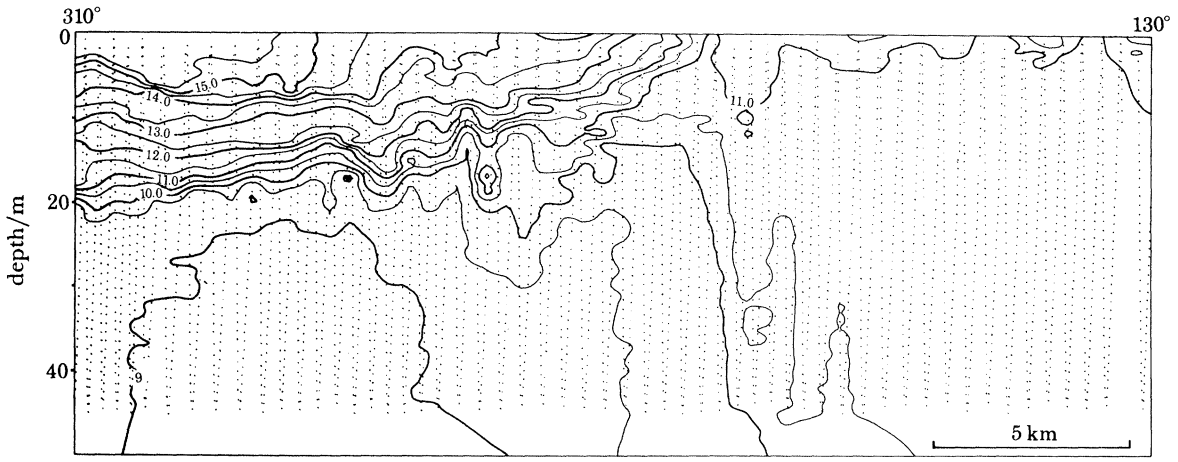

Figure 4. High resolution temperature section of the western Irish Sea front. Dots represent data points from the undulating CTD system which described a vertical cycle in a horizontal distance of *ca.* 500 m. Salinity variations measured at the same time were small, not exceeding ± 0.1 ‰.

Stratification of the water column is characterized by the potential energy anomaly ϕ† defined as

$$\phi = \frac{1}{h}\int_{-h}^{0} (\bar{\rho} - \rho)\, gz \, \mathrm{d}z; \quad \bar{\rho} = \frac{1}{h}\int_{-h}^{0} \rho \, \mathrm{d}z.$$

The anomaly ϕ is the amount of work per unit volume required to bring about vertical redistribution of the mass in complete mixing. Where surface heating is the only stabilizing input and stirring is due to wind and tidal stresses, the changes in ϕ may be written, for zero advection (Simpson *et al.* 1978), as

$$\frac{\mathrm{d}\phi}{\mathrm{d}t} = \frac{\alpha g \dot{Q}}{2c} - \epsilon k_{\mathrm{b}} \rho \overline{|\boldsymbol{u}_{\mathrm{b}}|^3} - \delta k_{\mathrm{s}} \rho_{\mathrm{s}} \frac{\overline{W^3}}{h}, \tag{1}$$

† Equivalent to $-\overline{V}$ in previous work.

where α is the volume expansion coefficient; $\dot{Q}$ the surface heating rate; c the specific heat; $\boldsymbol{u}_b$ the tidal stream velocity near the seabed; k_b the drag coefficient associated with $\boldsymbol{u}_b$; W^3 the mean cube of the windspeed close to the sea surface; k_s the appropriate surface drag coefficient $\times \gamma$; γ the ratio of wind-induced surface current to wind speed; and ϵ, δ are the efficiencies of mixing by tide and wind respectively.

Where the tidal streams are approximately rectilinear we may write $\overline{|\boldsymbol{u}_b|^3} = \frac{4}{3}\pi U_b^3$, where U_b is the amplitude of the tidal stream.

Since negative values of ϕ would correspond to unstable conditions, ϕ is restricted to positive values only. The point where $\mathrm{d}\phi/\mathrm{d}t$ becomes equal to zero defines the frontal position and is given by

$$B = \frac{\alpha g \dot{Q}}{2c} = \frac{4}{3\pi}\epsilon k_b \rho \frac{U_b^3}{h} + \delta k_s \rho_s \frac{\overline{W^3}}{h} \qquad (2)$$
$$= M + N.$$

When the tide-mixing term M predominates, equation (2) simplifies to

$$\frac{3\pi\alpha g}{8\epsilon k_b \rho c}\left(\frac{\dot{Q}h}{\overline{U_b^3}}\right) = 1 \qquad (3)$$

The determination of h/U^3 is greatly facilitated by the use of numerical hydrodynamic models of the tidal flow that determine the depth mean velocity $\boldsymbol{u}$. A particularly useful model for this purpose is that developed by Pingree & Griffiths (1978) which covers much of the European shelf with a resolution of *ca.* 10 km. The resulting $h/|\boldsymbol{u}|^3$ map serves as an excellent reference and represents a significant improvement on previous estimates (Simpson *et al.* 1977) based on tidal atlas compilations of the surface tidal stream amplitudes at springs.

Wind-mixing also contributes to the control of stratification and fronts but its influence is generally less pronounced. This is because the time-average of W^3 is spatially relatively uniform so that, although the rate of input of energy by the wind-stress is significant, the *pattern* of stratification is determined by tidal stirring as represented by u^3/h which shows a large range of variation. The contribution of the W^3/h term for the U.K. shelf area has been investigated by regression analysis of the observed distribution (Simpson *et al.* 1978).

Studies of other areas high in tidal energy, like the Bay of Fundy (Garrett *et al.* 1978), the Bering Sea (Schumacher *et al.* 1979), and the Cook Strait, New Zealand (Bowman *et al.* 1980) show similar behaviour. Even in a relatively low energy environment in the Gulf of St Lawrence Pingree & Griffiths (1980) find evidence of tidal-mixing effects corresponding to the h/u^3 predictions of their numerical model.

(*b*) *Predictions of frontal movement*

With the efficiencies ϵ and δ held constant, equation (1) may be integrated forward in time from the onset of stratification to give a prediction of frontal movement in response to the seasonal heating cycle and variations in tidal mixing. We represent the latter by a simple springs–neaps cycle for the tidal stream amplitude U_b given by

$$U_b = u_2(1 + e\cos\sigma t), \quad \sigma = 2\pi/14.5\,\mathrm{rad\,day^{-1}}.$$

Choosing $e = 0.3$ gives a springs:neaps ratio typical of the Irish Sea. The buoyancy input is represented by a seasonal function of the form

$$\dot{Q} = Q_0 \cos(\omega t + \psi),$$
$$Q_0 = 140\,\mathrm{J\,m^{-2}\,s^{-1}}, \quad \omega = 2\pi/365\,\mathrm{day^{-1}}.$$

A prediction based on these assumptions is found to exhibit marked oscillations in frontal positions over the fortnightly cycle (figure 5).

The effect of stored buoyancy, accumulated during the low energy part of the mixing cycle, restricts the frontal movement so that the ratio of mixing powers at neaps and springs positions is just (Simpson & Bowers 1981)

$$P_n/P_s = (2+3e^2)/[2(1-e)^3] = 3.31 \quad (\text{for } e = 0.3) \tag{4}$$

which is just over half (52 %) of the 'equilibrium adjustment'.

Even so the predicted movement is still considerably greater (by a factor of *ca.* 2.5) than that deduced from observations (figure 2). This discrepancy has led to consideration of variable efficiency models (Simpson & Bowers 1981) in which ϵ and δ are made to vary with ϕ according to:

$$\frac{\epsilon}{\epsilon_0} = \frac{\delta}{\delta_0} = \left(\frac{C}{C+\phi}\right)^{\frac{1}{2}}, \tag{5}$$

where ϵ_0, δ_0 and C are constants. The ratio ϵ/ϵ_0 decreases with increasing ϕ until $\epsilon/\epsilon_0 = 0.25$ after which it is held constant.

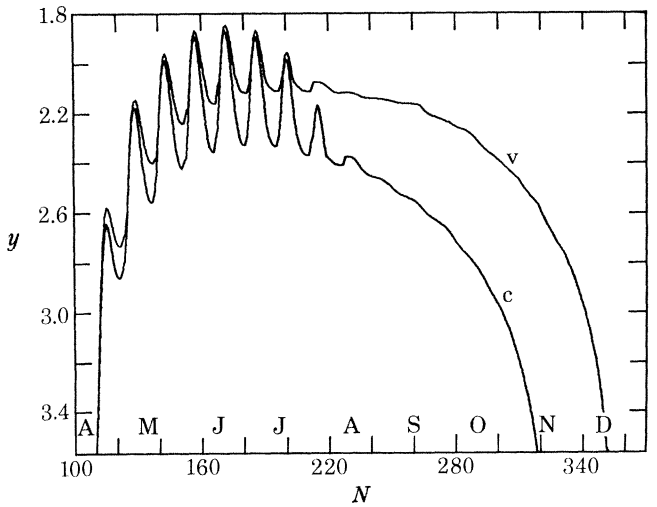

FIGURE 5. Comparison of the predictions of frontal movement from constant (c) and variable (v) efficiency models. Results are displayed as the value of $y = \lg h/u^3$ for marginal stratification ($\phi = 1\,\mathrm{J\,m^{-3}}$) plotted against day number N. Note the reduced response of the variable efficiency model to springs–neaps forcing, and its prediction of very limited movement in mean position between days 140 and 260 (May–September).

The prediction based on this formulation is also shown in figure 5 and represents an improvement on the constant-efficiency model in several respects. The neaps–springs oscillation is reduced to a level that agrees with observation (figure 2). At the same time, the incorporation of feedback accelerates the spread of stratification in the spring and gives rise to a period of nearly constant frontal positions from early June to late August, which is also consistent with observations. In addition it increases the 'sharpness' of the fronts relative to the constant-efficiency model and this too corresponds with the observed ϕ distributions at fronts. It is shown, for example, in Allen *et al.* (1980) that ϕ varies more rapidly than u^3/h so that the apparent efficiency of mixing, ϵ, decreases markedly with increasing stratification.

4. The relation of fronts to circulation

(a) *Contribution to the mean flow*

Residual flows in the shelf seas are generally much less than the tidal streams and often so small that they are difficult to determine. For the Irish Sea, application of the hydrographic theorem to the salinity distribution (Bowden 1955) and the ^{137}Cs data (Wilson 1974) indicate a mean northwards flow of *ca.* 0.3 cm s^{-1}. A similarly low level of long term mean advection is suggested by the study of flow in the north channel based on cable voltages (Bowden & Hughes 1961).

Mean velocities determined by current meters are frequently larger than this but when the averaging period is increased to one month or longer, the mean velocities decrease to a level of typically 1–2 cm s^{-1} which is close to the noise level of even the best current-measuring systems (Booth 1978).

Against this background of generally weak residuals, the contribution of the baroclinic flow along fronts may be significant. As indicated in § 2 (*b*), the geostrophic velocities associated with the observed density field may be *ca.* 20–30 cm s^{-1} in the frontal jet, and according to the dynamic model of James (1977), this flow is only slightly reduced by the effects of friction. So, if fronts were stable, they would make an important though rather localized contribution to the mean kinetic energy with velocities up to ten times that of the background.

As we have noted, however, fronts are prone to instabilities that result in a much more complicated and time-varying velocity field at the front. There are indications that the non-tidal kinetic energy is greater in the frontal zones (Simpson *et al.* 1978) but there is a clear need for an objective study of all shelf-sea current meter data to assess the contribution of fronts and other candidate mechanisms like the effects occurring near headlands due to rectification of tidal flows.

(b) *Influence of the mean flow on fronts*

It will be apparent from the discussion of § 3 that a satisfactory first-order account of the distribution of stratification and fronts can be given in terms of models of vertical mixing alone without any allowance for advective effects. This clearly implies a restriction on the magnitude of the residual advection, at least in the direction perpendicular to the isolines of ϕ. To illustrate this point we now proceed to modify the mixing model to allow for the effects of advection by a residual current $\bar{\boldsymbol{u}}$ which we assume is uniform with depth. In doing so, it is necessary to consider changes in the potential energy anomaly of a particle as it moves over varying bathymetry. Vertical stretching or compressing of the water column in depth-uniform flow will not modify the *shape* of the density profile, so in terms of $\zeta = z/h$ we have

$$\phi = gh \int_{-1}^{0} (\bar{\rho} - \rho)\, \zeta \, \mathrm{d}\zeta$$

and

$$\mathrm{d}\phi/\mathrm{d}h = \phi/h.$$

The total rate of change of ϕ following a particle may then be written as

$$\begin{aligned} \mathrm{D}\phi/\mathrm{D}t &= \partial\phi/\partial t + \bar{\boldsymbol{u}}\cdot\nabla\phi \\ &= B - M - N + (\phi/h)\, \bar{\boldsymbol{u}}\cdot\nabla h. \end{aligned} \tag{6}$$

Advection will be negligible only if the leading terms B and M swamp the contribution from $\bar{\boldsymbol{u}}$ so that for example

$$B \gg |\bar{\boldsymbol{u}}\cdot\nabla\phi|$$

PHILOSOPHICAL TRANSACTIONS OF THE ROYAL SOCIETY A MATHEMATICAL, PHYSICAL & ENGINEERING SCIENCES

which implies that the normal velocity component u_n must satisfy

$$|u_n| \ll \frac{B}{|\nabla\phi|} \approx \frac{4}{2\times10^{-3}}\left[\frac{\mathrm{J\,m^{-3}\,d^{-1}}}{\mathrm{J\,m^{-4}}}\right] \approx 2\,\mathrm{cm\,s^{-1}}$$

for a typical frontal gradient. Such a restriction is not inconsistent with the generally low levels of residual velocities already noted.

In principle the influence of advection on a frontal zone can be found by solving equation (6) for given buoyancy and mixing inputs together with a specified form of $\bar{u}$. As the simplest example illustrating the frontal response we consider the flow over a symmetrical ridge (figure 6). Both the tidal and the mean flow are orthogonal to the ridge. The tidal transport has an amplitude T_2 which, like the residual transport T_0, is independent of position. With these assumptions and $N = 0$, the distribution of $\phi(x)$ at time t is found by integrating equation (6) for individual particles as they move over the ridge.

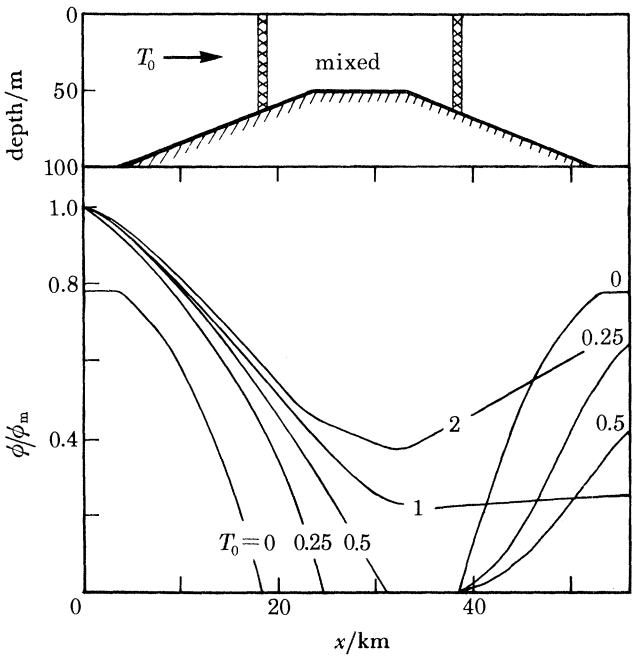

FIGURE 6. Predictions based on equation (6) of the distribution of the potential energy anomaly ϕ in depth-uniform flow over a ridge. $T_0/\mathrm{m^2\,s^{-1}}$ represents the (constant) transport in the mean flow so that $T_0 = 0.5\ \mathrm{m^2\,s^{-1}}$ corresponds to a flow of 1 cm s^{-1} on the ridge. Time of prediction is $t = 182$ days (summer solstice).

Results at the time of maximum heat input are shown in figure 6 for different values of the residual transport, together with the no-advection case. With a transport of $T_0 = 0.25\,\mathrm{m^2\,s^{-1}}$, equivalent to a mean velocity on the ridge of 0.5 cm s^{-1}, the frontal position is markedly displaced on the upstream side of the ridge. The re-establishment of stratification on the downstream side commences at the same point as in the no-advection case but the spatial gradient of ϕ is reduced.

Further increase in T_0 accentuates these effects, with the stratified water extending further over the ridge, until at $T_0 \approx 1\,\mathrm{m^2\,s^{-1}}$ the mixed region is eliminated. At high values of T_0 the ridge will produce only a weak minimum in the distribution displaced in the direction of the current.

This simple model confirms the sensitivity of the structure to very small residual flows and

suggests that we might examine observed distributions for evidence of displacement by the mean current. Generally the available data indicate a close alignment of ϕ and h/u^3 contours, which would again point to low levels of mean circulation, but comparison of long term mean frontal positions with accurate h/u^3 data may reveal exceptions. Figure 7 shows the mean position of the Islay front based on i.r. images along with the h/u^3 contours derived from the Pingree &

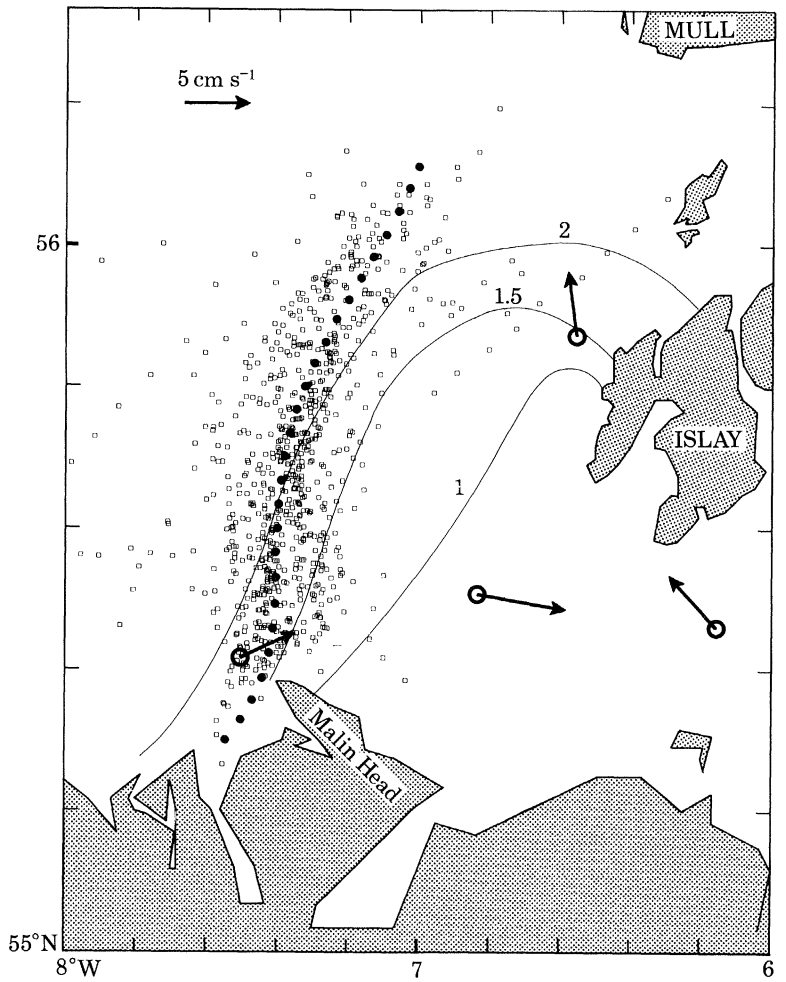

FIGURE 7. Mean position of the Islay front (solid circles) based on observed positions (open squares) from satellite i.r. imagery over the period August 1976–June 1980. Arrows represent the vectors of mean velocities averaged over about 1 month. Note the bending of the mean frontal curve relative to the contours of lg h/u^3, which are based on the model of Pingree & Griffiths (1978), and the apparent disappearance of the front northwest of Islay.

Griffiths model. Immediately to the north of Malin Head the average frontal position is significantly displaced to the east of the contour lg $h/u^3 = 2$. Further north, the front is found at higher h/u^3, while to the north of Islay the absence of observed fronts suggests a weakening of the gradients associated with a mean flow from the mixed to the stratified side of the front. These features are consistent with the residual flow in the area as indicated by a recent current meter survey by I.O.S. (J. Howarth, personal communication). The vectors shown in figure 7 are the average flows over a period about 1 month. They show evidence of an eastward flow off

Malin Head of *ca.* 5 cm s^{-1} with an inflow to the Irish Sea on the west side of the channel, and a northward flow along the Scottish coast which we may interpret as being responsible for the disruption of the front which fails to follow the h/u^3 contours to the northwest of Islay.

(*c*) *Frontal zones around islands*

As a second example of the effects of the mean flow we now consider an island in a stratified sea. The island is assumed to be a cylinder located in water of constant depth. Away from the perturbing influence of the island, the tidal ellipse is degenerate and its axis is assumed to be parallel to that of the mean flow $\bar{u}$. The influence of the island on both tidal and mean flow is represented by the well known potential flow solution for a cylinder.

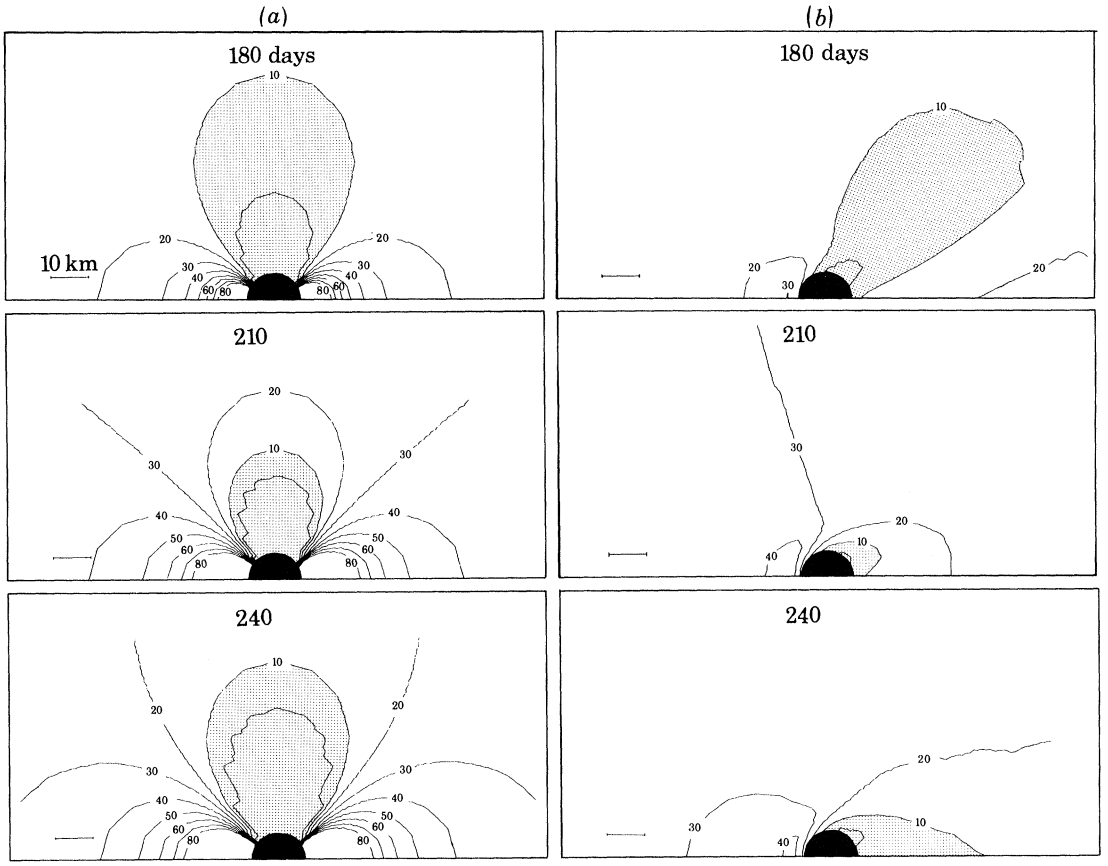

FIGURE 8. Solutions of equation (6) for a cylindrical island in a stratified sea. Results are shown in terms of contours of ϕ (J m^{-3}) at different stages of the heating cycle for: (*a*) the reference case of zero advection, (*b*) a mean flow (from left to right) of $\bar{u} = 2.5$ cm s^{-1} and a diffusion coefficient $K_x = 35$ m^2 s^{-1}.

With these assumptions equation (6) has been solved numerically by M. Argote Espinoza to predict the distribution of ϕ during the seasonal heating cycle. For zero advection (figure 8*a*) the distribution of ϕ essentially reflects that of h/u^3 so that minima occur on the flanks of the island where the tidal flow is forced to accelerate. This pattern of asymmetric mixing around the island is also apparent in a full dynamical model of the tidal flow past a more realistic island (Pingree & Maddock 1979).

Figure 8*b* shows the result for a mean flow of 2.5 cm s^{-1}. At day 180 (mid-summer) the low stability 'wings' of the distribution are displaced in the direction of the current. By day 210

the contrast with the no-advection case is even more marked as the lower stability regions ($\phi < 10\,\mathrm{J\,m^{-3}}$) are swept behind the island to merge into a single low stability wake region as the heating decreases (day 240).

Evidence of such wake development can be seen in a few i.r. images of the Scilly Isles which, for example in the period 18–20 August 1976, suggest cold water streaming northwards from the islands (figure 9, plate 2). The coldest surface water is in two centres slightly 'downstream' of the islands. This basic asymmetry of the distribution of stratification around the island has been confirmed in ship observations of the temperature–salinity structure around the Scilly Isles during July 1979, details of which will be reported elsewhere.

5. Discussion

From the increasing weight of observational evidence, we now have a clear picture of the fronts as major structural features of the shelf seas during the summer months. The mean positions of the fronts are described by h/u^3, and this parameter should serve well as a general index of vertical mixing. For biological purposes it has been suggested by Pingree *et al.* (1978) that the relevant physical characteristics of frontal zones may be represented by h/u^3 and its spatial gradient, along with a parameter $H = Kh$ (where K = diffuse attenuation coefficient) which represents the extent of natural light penetration.

Detailed studies of frontal behaviour, however, show up features, particularly the lack of springs–neaps adjustment, that are not in accord with the constant efficiency model. A substantially improved account of frontal movements can be given in terms of models, like that of § 3, that incorporate some feedback.

This is not surprising since, as has recently been pointed out by Hopfinger & Linden (1981), the relevant energy level is that occurring near the surface, where the buoyancy is input, so that the *decay* of turbulence generated near the bottom should enter the problem and lead to an additional depth dependence. Hopfinger & Linden have investigated the development of stratification in response to heating in a grid-stirred tank and observed behaviour qualitatively similar to that observed in the ocean. They find that the onset of stratification in a previously mixed system may be predicted from a criterion analogous to $\dot{Q}h/u^3$. For established stratification, however, the mixing rate is dependent on existing density gradients which in turn are functions of the previous heating and stirring history. A feature of this dependence in the ocean seems to be the relative difficulty of passing back from stratified to mixed conditions, and further investigation of this reverse transition in tank experiments seem desirable. Coexisting with this ordered structure of mixed, stratified and frontal zones is the pattern of mean circulation. All the indications are that these mean flows are generally weak.

The observed consistency of frontal positions itself implies severe constraints on the mean circulation. The two examples considered above illustrate the sensitivity of the density structure even to weak advective flows normal to the frontal zones. The implication is clearly that cross-frontal velocities are small and that any mean flow should be parallel to the front. This would also be a requirement for a front's internal baroclinic flow if there is a geostrophic balance with the density gradients set up by mixing processes.

The observational data available however do not clearly identify strong along-front flows except in a few particular cases. This points to the influence of eddy instabilities which disrupt the frontal structure and produce a complicated time-dependent velocity field in the frontal zone.

PHILOSOPHICAL TRANSACTIONS OF THE ROYAL SOCIETY A MATHEMATICAL, PHYSICAL & ENGINEERING SCIENCES

They may also be responsible for the apparently random fluctuation in frontal positions that remains after the removal of the tidal advection and the springs–neaps cycle.

The sensitivity of frontal position and structure to mean flow suggests that anomalies in frontal position relative to the h/u^3 contours may provide a useful diagnostic for the existence of a cross-frontal mean flow, as in the case cited of the Islay front, whose distortion seems to point to the existence of a Scottish coastal current.

I am grateful to John Howarth of I.O.S. Bidston for kindly providing the residual velocity data shown in figure 7. David Bowers and Maria Luisa Argote Espinoza gave much valuable help with numerical calculations and the preparation of diagrams. The satellite imagery was made available by P. Baylis and J. Brush of the University of Dundee.

References (Simpson)

Allen, C. M., Simpson, J. H. & Carson, R. M. 1980 *Oceanologica Acta* **3** (1), 59–68.
Booth, D. 1978 Ph.D. thesis, University of Wales.
Bowden, K. F. 1955 The Physical Oceanography of the Irish Sea. *Fishery Invest., Lond. Ser.* II, **18** (8).
Bowden, K. F. & Hughes, P. 1961 *Geophys. Jl R. astr. Soc.* **5** (1), 265–291.
Bowman, M. J., Kibblewhite, A. C. & Ash, D. E. 1980 *J. geophys. Res.* **85** (C5), 2728–2742.
Dietrich, G. 1951 *Nature, Lond.* **168**, 8–11.
Garrett, C. J. R., Keeley, J. R. & Greenberg, D. A. 1978 *Atmosphere - Ocean* **16** (4), 403–423.
Green, J. S. A. 1970 *Q. Jl R. met. Soc.* **96**, 157–185.
Hopfinger, E. & Linden, P. F. 1981 *J. Fluid Mech.* (Submitted.)
James, I. D. 1977 *Estuar. coast. mar. Sci.* **5**, 339–353.
James, I. D. 1978 *Estuar. coast. mar. Sci.* **7**, 197–202.
Matthews, D. J. 1913 The salinity and temperature of the Irish Channel and the waters south of Ireland. *Scient. Invest. Fish. Brch Ire.* **4**, 1–26.
Pingree, R. D., Holligan, P. M. & Head, R. N. 1977 *Nature, Lond.* **265**, 266–269.
Pingree, R. D. 1978 *J. mar. biol. Ass. U.K.* **58**, 955–963.
Pingree, R. D., Holligan, P. M. & Mardell, G. T. 1978 *Deep Sea Res.* **25**, 1011–1028.
Pingree, R. D. & Maddock, L. 1979 *J. mar. biol. Ass. U.K.* **59** (3), 699–710.
Pingree, R. D. & Griffiths, D. K. 1978 *J. geophys. Res.* **83** (C 9) 4615–4622.
Pingree, R. D. & Griffiths, D. K. 1980 *Oceanologica Acta* **3**(2), 221–225.
Schumacher, J. D., Kinder, T. H., Pashinski, D. J. & Charnell, R. L. 1979 *J. phys. Oceanogr.* **9**, 79–87.
Simpson, J. H. & Hunter, J. R. 1974 *Nature, Lond.* **250**, 404–406.
Simpson, J. H., Hughes, D. & Morris, N. C. G. 1977 In *A voyage of discovery* (ed. M. Angel), suppl. to *Deep Sea Res.* pp. 327–340.
Simpson, J. H. & Pingree, R. D. 1978 *Oceanic fronts in coastal processes*, ch. 5. Berlin, Heidelberg, New York: Springer-Verlag.
Simpson, J. H., Allen, C. M. & Morris, N. C. G. 1978 *J. geophys. Res.* **83** (C9), 4607–4614.
Simpson, J. H. & Bowers, D. G. 1979 *Nature, Lond.* **280**, 648–651.
Simpson, J. H., Edelsten, D. J., Edwards, A., Morris, N. C. G. & Tett, P. B. 1979 *Estuar. coast. mar. Sci.* **9**, 713–726.
Simpson, J. H. & Bowers, D. 1981 *Deep Sea Res.* **28**(7), 727–738..
Wilson, T. R. 1974 *Nature, Lond.* **248**, 125–127.

Discussion

D. J. Crisp, F.R.S. (*N.E.R.C. Unit, Marine Science Laboratories, Menai Bridge, Gwynedd LL*59 5*EH*, U.K.). It is now well accepted that oceanic fronts influence the conditions, abundance and diversity of planktonic organisms. Recently I compared the coastal regions where stratified water exists in summer with those where the coastal water is continuously mixed, and found that there was a significant relation with certain intertidal species.

The clearest relations can be seen for organisms whose reproduction is thought to depend on elevated summer temperatures, and that are adapted to water of low turbidity. Such species in

PHILOSOPHICAL TRANSACTIONS OF THE ROYAL SOCIETY A MATHEMATICAL, PHYSICAL & ENGINEERING SCIENCES

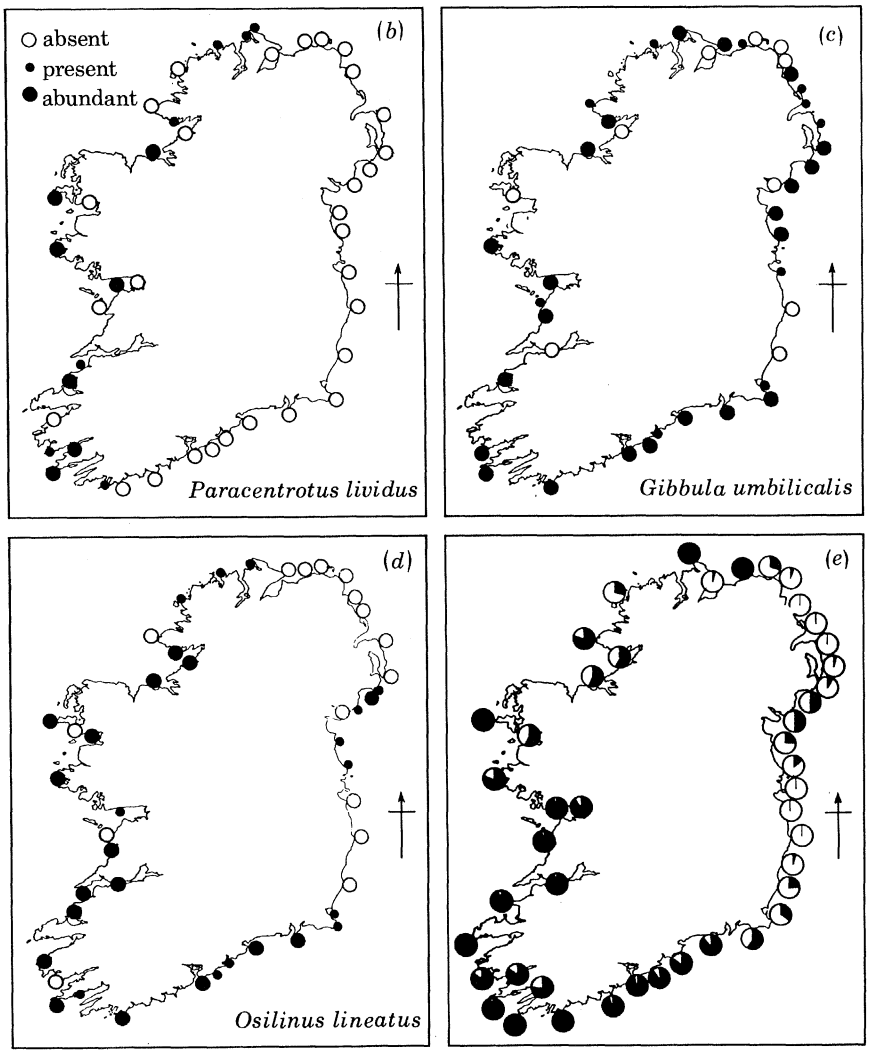

FIGURE D 1. (*a*) Satellite picture of Ireland showing stratified water (dark) and mixed water (light). (*b*) Distribution of *Paracentrotus lividus*. (*c*) Distribution of *Gibbula umbilicalis*. (*d*) Distribution of *Osilinus lineatus*. (*e*) Pie diagram of relative abundance of *Chthamalus* sp. (black) and *Balanus balanoides* (white). (The maps were first published in Crisp & Southward (1954).)

PHILOSOPHICAL TRANSACTIONS OF THE ROYAL SOCIETY A MATHEMATICAL, PHYSICAL & ENGINEERING SCIENCES

the North Atlantic area are called 'Lusitanian' and are found at the western borders of Europe and in the Mediterranean. They reach their limits around the coasts of Ireland and Scotland.

One would therefore expect their abundance to show a positive correlation with areas of summer stratification and a negative correlation with cooler mixed water (figure D 1 (*a*)).

The first map (figure D 1 (*b*)) shows the Lusitanian urchin, *Paracentrotus lividus*, confined to the warmer waters to the west of Ireland and cut off at the front close to Malin Head at the northerly tip of Donegal, and to the south near Cork.

The second map (figure D 1 (*c*)) shows a very temperature-tolerant species, the topshell *Gibbula umbilicalis*, which extends much further north into Shetland. It clearly shows a reduction in abundance in regions of mixed water, and an increase in abundance in southern County Down adjacent to the western Irish Sea front.

The third map (figure D 1 (*d*)) shows the ratio of the abundance of the barnacle genus *Chthamalus*, a summer breeder, to that of *Balanus balanoides*, a subarctic winter breeder occupying the same habitat. The distribution is similar to that of the previous map, showing that warm stratified water influences *Chthamalus* but not *Balanus* when other physical influences, affecting both species, are eliminated. The last map (figure D 1 (*e*)), that of the topshell, *Monodonta lineata*, clearly picks out regions of stratified water, and avoids mixed water. These distributions were published in 1954 (Crisp & Southward 1954), long before explanations in terms of fronts were available, and hence we could not comment on this close correlation at that time.

It would be interesting to know whether bottom-living animals respond to differences in water temperature at fronts, though at the bottom, of course, it would be mixed water that would favour warmer-water species.

Reference

Crisp, D. J. & Southward, A. J. 1954 *Proc. R. Irish Acad.* **57**, § B, no. 1 (29 pp.).

C. Hearn (*CSIRO Fisheries & Oceanography, Marmion, Western Australia, and Environmental Dynamics, University of Western Australia*). I have just completed a theoretical study of boundary fronts using the ideas of the rapidly developing field of synergetics (Haken 1978). The non-equilibrium driving force is the surface-heating of the water column, and this can be represented by a control parameter $\Gamma \equiv \dot{Q}h/u^3$. If Γ exceeds a critical value Γ_c the mixed state cannot be maintained (for long times) and a non-equilibrium phase transition takes place to create the highly ordered, low energy, stratified phase. The limited régime of the mixed phase, and the self-organizational processes that regulate the stratified phase, stem from the nonlinear behaviour of the eddy diffusivity which is governed by the available turbulent kinetic energy (t.k.e.). Stratification nucleates near a critical point in the water column that is determined by the vertical variation of t.k.e. Simple models of this distribution gives values of Γ_c in accord with the efficiencies of tidal and wind mixing deduced by Simpson & Bowers (1981). The stratified phase is highly stable, owing to the reduction in t.k.e. by the stratification, and so the water column does not return to the mixed phase when Γ is reduced below Γ_c, and only prolonged surface cooling can destroy the ordered phase. The self-organization maintains a discontinuity in the temperature gradient at the top of the lower, tidally mixed, layer by adjusting the thermal structure of the upper water column to accommodate both the daily variations and fluctuations in surface heating and the large changes in wind-stirring. The theory predicts that, in the absence of cross-frontal mixing, the only movement occurring after the summer maximum heating will be tidal advection.

PHILOSOPHICAL TRANSACTIONS OF THE ROYAL SOCIETY A MATHEMATICAL, PHYSICAL & ENGINEERING SCIENCES

It also indicates that the Simpson–Hunter h/u^3 criterion should be based on the neaps tidal stream velocity, but this modification does not significantly affect the predicted frontal positions.

References

Haken, H. 1978 *Synergetics*. Berlin: Springer-Verlag.
Simpson, J. H. & Bowers, D. 1981 *Deep-Sea Res.* **28**(7), 727–738.

PHILOSOPHICAL TRANSACTIONS OF THE ROYAL SOCIETY A MATHEMATICAL, PHYSICAL & ENGINEERING SCIENCES

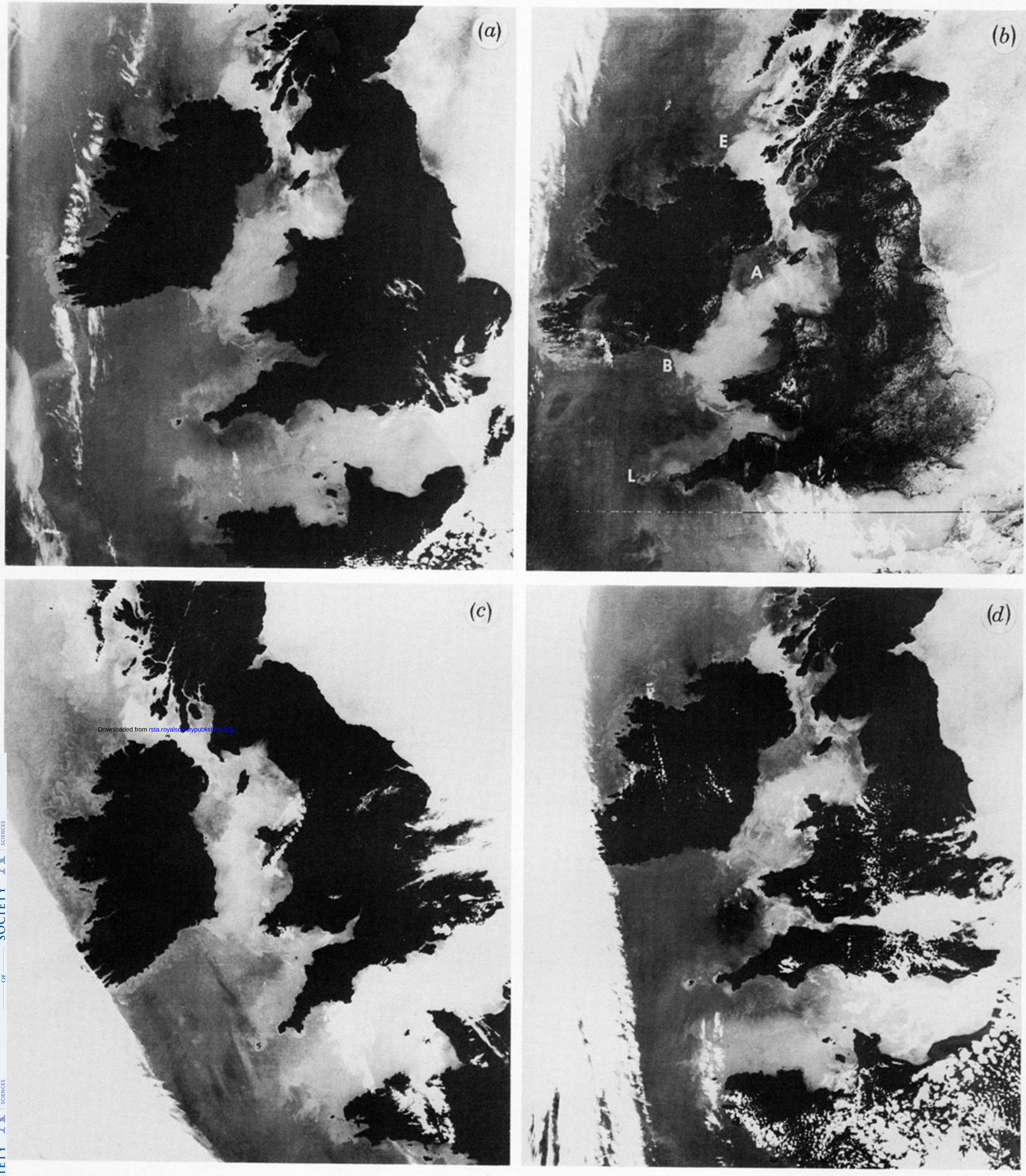

FIGURE 1. Satellite infrared images of the U.K. shelf area in May 1980. (*a*) TIROS–N, 16.v.80, 15h29 G.M.T.; (*b*) NOAA–6, 16.v.80, 19h01 G.M.T.; (*c*) NOAA–6, 17.v.80, 08h49 G.M.T.; (*d*) TIROS–N, 17.v.80, 15h18 G.M.T.

Letters on (*b*) indicate the principal frontal zones referred to in the text: A, western Irish Sea front; B, Celtic Sea front; E, Islay front; L, Scilly Isles.

PHILOSOPHICAL TRANSACTIONS OF THE ROYAL SOCIETY A MATHEMATICAL, PHYSICAL & ENGINEERING SCIENCES

FIGURE 9. Enlarged satellite infrared image of the Scilly Isles region from NOAA–5 at 10h28 G.M.T. 20.viii.76.

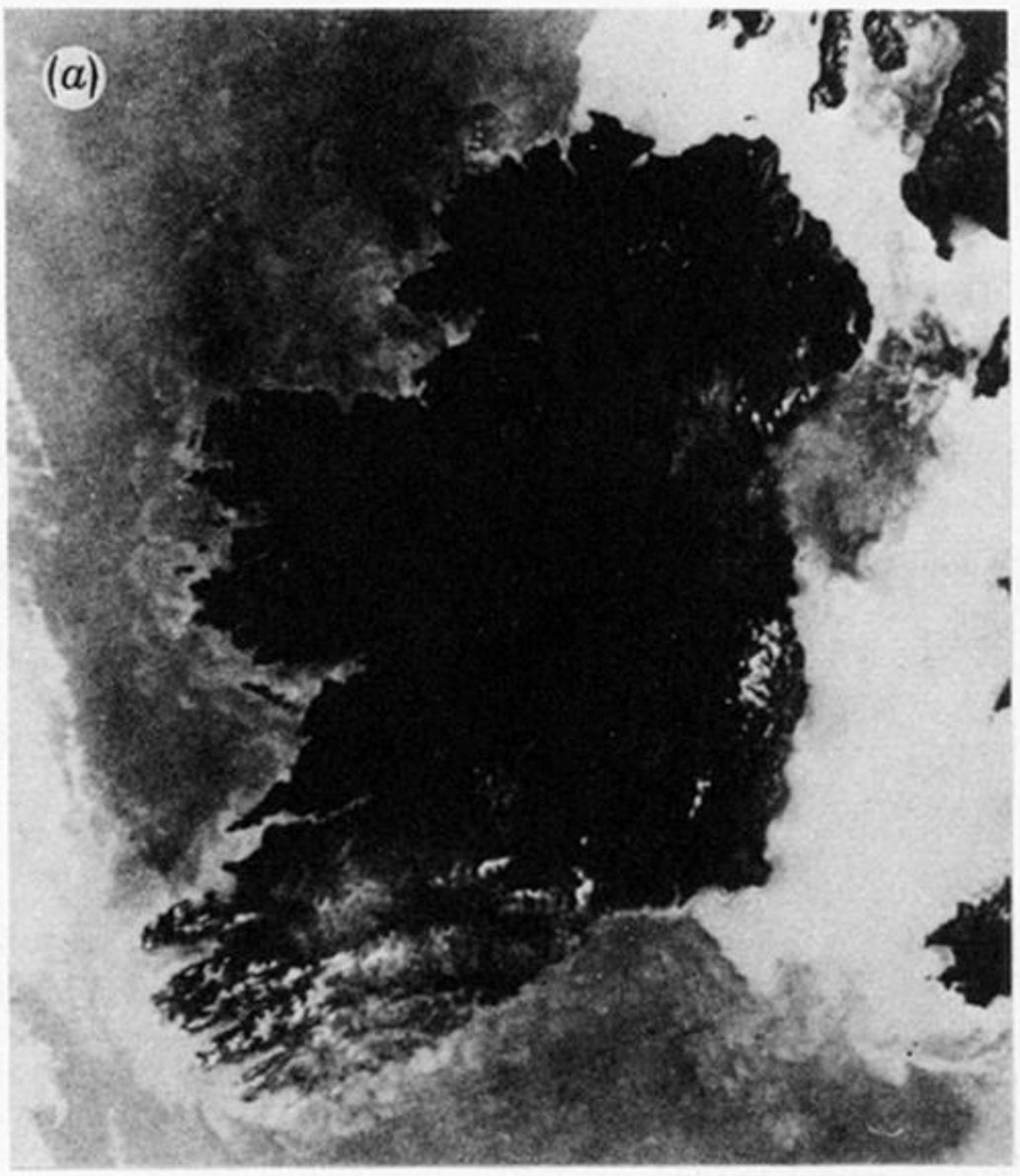

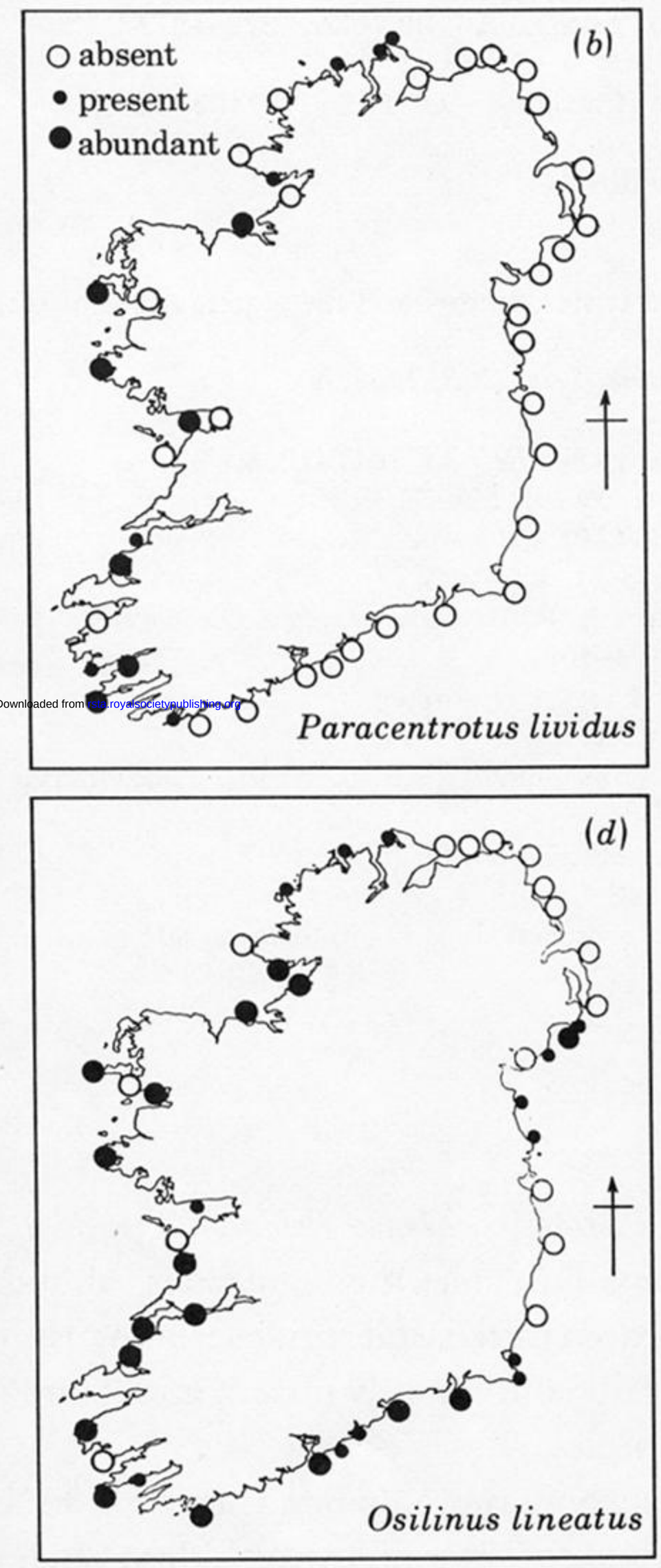

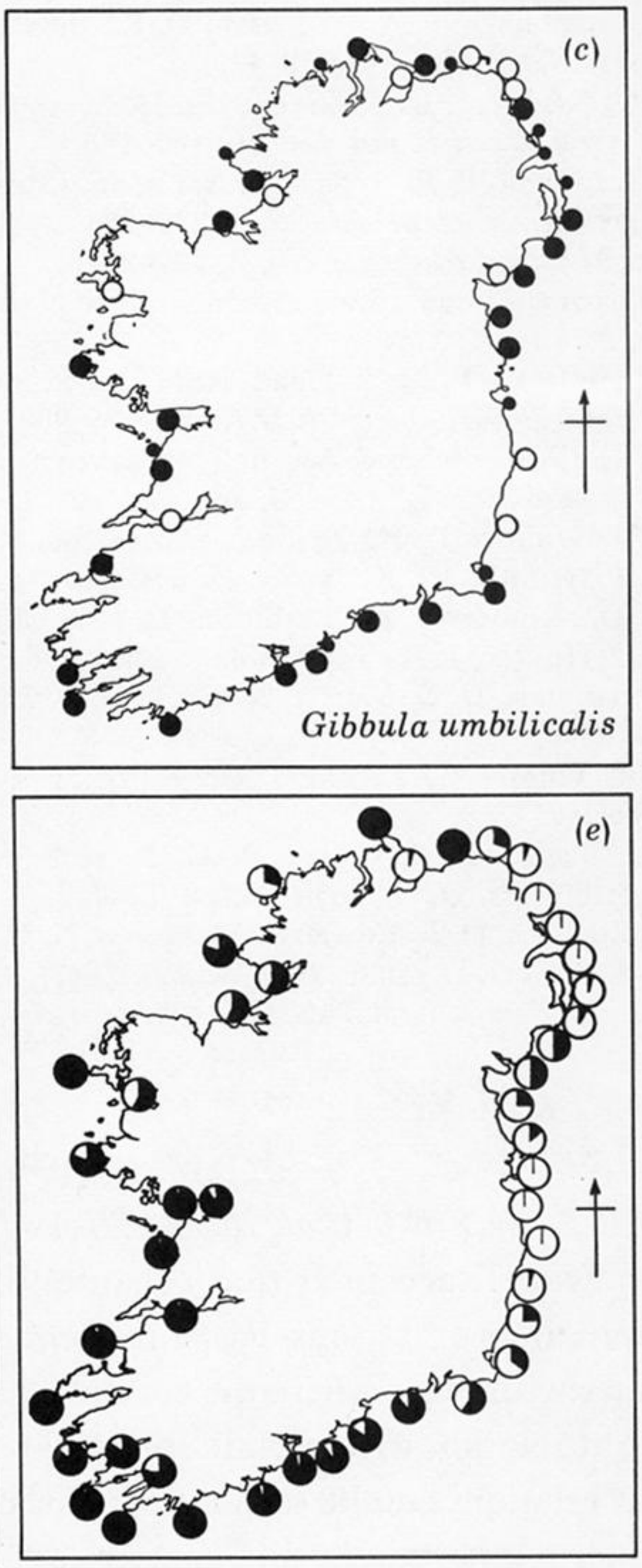

FIGURE D 1. (*a*) Satellite picture of Ireland showing stratified water (dark) and mixed water (light). (*b*) Distribution of *Paracentrotus lividus*. (*c*) Distribution of *Gibbula umbilicalis*. (*d*) Distribution of *Osilinus lineatus*. (*e*) Pie diagram of relative abundance of *Chthamalus* sp. (black) and *Balanus balanoides* (white). (The maps were first published in Crisp & Southward (1954).)